Soil-Foundation Interaction Behavior of Highway Guardrail Posts

JEY K. JEYAPALAN, JAMES F. DEWEY, Jr., T. J. HIRSCH,
HAYES E. ROSS, Jr., and HAROLD COONER

ABSTRACT

The Texas State Department of Highways and Public Transportation uses two types of guardrail posts: a circular wood post and a steel W6x8.5 post. The current specifications require the steel post to be placed in a concrete footing. However, the concrete footing is not required for the wood post. Because of this requirement, the steel post guardrail systems are not considered to be as economical as the wood post guardrail system. The research study reported herein was conducted to determine whether the concrete footings are necessary for the steel guardrail posts to perform satisfactorily as a traffic barrier system. An analytical model was developed to model the guardrail post as a laterally loaded drilled shaft. This model represents the realistic behavior of drilled shafts under lateral loading conditions adequately, while being simple enough for use in day-to-day design of guardrail post foundations. A series of static load tests and dynamic impact tests was conducted to determine whether the steel guardrail post performs satisfactorily. The results of these tests indicate that the steel guardrail post, embedded without the concrete footing, performs similarly to the timber post. The results of these field tests were also used to verify the analytical model, and the agreement with the theoretical predictions was found to be satisfactory.

The primary function of guardrails and median barriers is to safely redirect errant vehicles. Guardrail installations on shoulders prevent vehicle access to steep embankments or fixed objects, whereas median barriers are used between the roadways of divided highways to prevent across-the-median collisions with opposing traffic. Properly designed installations accomplish the redirection of errant vehicles in such a manner as to minimize the vulnerability of vehicle occupants as well as the involvement of following and adjacent traffic.

When a vehicle in motion collides with a guardrail, a substantial portion of the energy of the vehicle is absorbed by the guardrail. The lateral forces carried by the guardrail are transmitted to the ground through the guardrail posts. Because the resistance and the subsequent energy loss are provided by the soil surrounding the guardrail posts, the soil properties at a site will determine the behavior of the guardrail posts. Although extensive research has been done on the efficiency of various types of guardrail systems as highway barriers, little work has been done on the influence of soil properties on the performance of guardrail posts.

The Texas State Department of Highways and Public Transportation (TSDHPT) currently uses two types of guardrail posts: a circular wood post and a steel W6x8.5 post. The current specifications require the wood post to have a minimum diameter of 7 in., a minimum overall length of 69 in., and a minimum embedment depth of 38 in., with the top of the wood post domed. A minimum overall length of 66 in. is required if the top of the wood post is beveled. The specifications do not require the wood post to be placed in a concrete footing.

The current specifications for the steel W6x8.5 guardrail post are the same as those for the beveled wood post with one exception: the steel post must be placed in a concrete footing. Because of this requirement for a concrete footing, the steel post guardrail systems are not as economical as the wood post guardrail systems. To date, no experimental work has been performed to determine whether the concrete footing is required for the steel post guardrail systems to perform satisfactorily as a traffic barrier. Any guardrail system that performed similarly to the system using wood posts would be considered as performing satisfactorily. With this in mind, a study was conducted to determine whether concrete footings are required for the steel guardrail posts to perform satisfactorily. The procedures used in conducting this study are as follows.

1. A computer model for laterally loaded guardrail posts are developed in which the guardrail post was modeled as a laterally loaded drilled shaft or pile.
2. Static field load tests were performed on steel and timber guardrail posts in two different soils.
3. The results from these static tests were used to compare the static behavior of the two types of posts. The results were also compared with the results generated from the computer model.
4. Dynamic field tests were performed on steel and timber guardrail posts in the soils used for the static tests.
5. The results from these dynamic tests were used to compare the dynamic response of the two types of posts. These results were also compared with the results predicted by the computer model.

SUMMARY OF PREVIOUS WORK

Field Tests on Guardrail Posts

Many crash tests have been performed on guardrail systems to determine the efficiency of these systems as highway barriers. Typically, these tests have concentrated on the damage to the rail and the vehicle, the redirection response of the vehicle, and the energy dissipation capability of the guardrail system. The vehicle redirection response and the energy dissipation characteristics of the system are influenced significantly by the soil conditions. However, the post-soil interaction behavior has never been studied in detail in these tests.

In 1970 Southwest Research Institute (1) conducted a study of the post-soil interaction behavior of highway guardrail posts. To evaluate the effects of soil conditions and embedment geometry, 72 tests were performed in two types of soils, with four embedment depths and three post widths. The results of these tests are as follows.

1. The dynamic resistance force (peak and average) and the kinetic energy absorbed by noncohesive soils are related to the shear strength of the soil.
2. The dynamic resistance force (peak and average) and the kinetic energy absorbed by the soil are directly related to the post width.
3. The dynamic resistance force (peak and average) and the kinetic energy absorbed by the soil are significantly affected by and directly related to the post embedment depth. The embedment depth has a more pronounced influence on post-soil system properties for soils with higher shear strength.
4. The dynamic resistance force (peak and average) and the kinetic energy absorbed by the soil are greater than the static resistance force (peak and average) and the energy absorbed by the soil.

This study clearly demonstrated that the performance of a highway guardrail system is significantly influenced by the post-soil interaction characteristics of the system.

Theoretical Analysis of Laterally Loaded Shafts or Piles

The soil-structure interaction behavior of guardrail posts can be analyzed by considering that the guardrail post behaves as a laterally loaded pile. Various methods of analysis are currently used for laterally loaded pile design. Some methods permit the pile foundation to reach some percentage of its ultimate capacity at the maximum foundation load. Other methods assume elastic foundation behavior up to the ultimate load. There are methods that limit soil pressures as determined from elastic analysis to allowable values, whereas still other methods are designed to meet certain deflection or rotation criteria at various load levels. Regardless of the design method used, the pile must be safe against both structural collapse and soil failure (excessive pile deflection or rotation or both).

The approaches used in pile design can be classified into three categories:

1. Ultimate lateral capacity models,
2. Linear load-deflection models, and
3. Nonlinear load-deflection models.

Further details of these models are discussed in Dewey et al. (2).

STATIC LOAD TESTS

The static guardrail post tests that were conducted are summarized in the following table:

Test No.	Post Type	Embedment Depth (in.)	Height of Load (in.)	Soil Type
1	Wood	38	21	Cohesive
2	Steel	38	21	Cohesive
3	Steel	44	21	Cohesive
4	Wood	38	21	Cohesionless
5	Steel	38	21	Cohesionless
6	Steel	44	21	Cohesionless

Three tests were performed in each soil type, one using a standard timber post and two using steel posts. The two tests on the steel posts were performed with different embedment depths in order to bracket the response of the timber post.

To assess the effects of varying soil conditions, the tests were performed in two soils with significantly different properties. A stiff cohesive soil and a cohesionless gravel were used for this purpose. The soil at the test site is a stiff cohesive soil, thus only one soil pit had to be constructed of gravel material. The test setup and the location of the posts are shown in Figures 1 and 2.

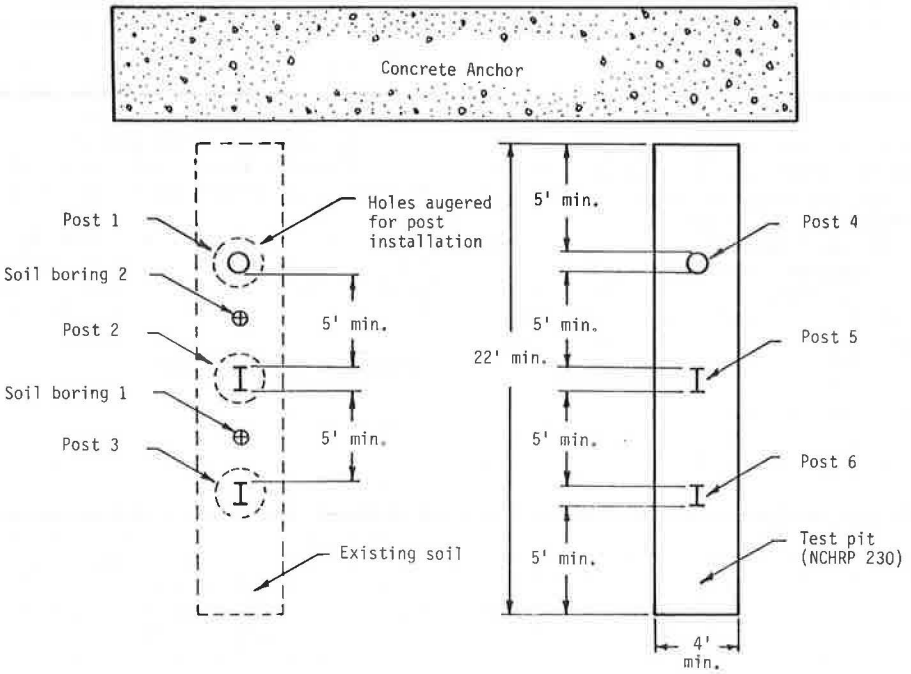

FIGURE 1 Location of posts.

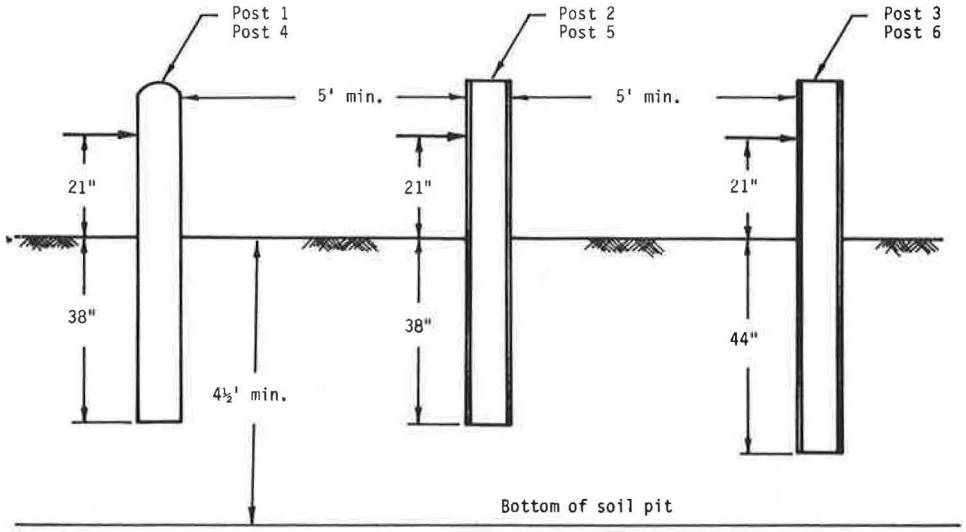

FIGURE 2 Placement of posts.

The posts were placed in the cohesive soil by augering and tamping the soil around the post. A 24-in.-diameter auger was used, and the soil was tamped around the posts in several lifts. In a cohesionless soil, however, augering is difficult because of the soil caving into the augered hole. Thus after the excavation of the pit the posts were held in place with struts, and the gravel was placed and compacted around the posts.

For the cohesive soil, soil conditions at the test site were determined by using two soil borings. The boring locations are shown in Figure 1. Undisturbed soil samples were taken with a 2.0-in.-diameter thin-walled tube sampler. Laboratory tests on the undisturbed samples included Atterberg limits, moisture contents, unit weights, and triaxial compression tests to determine the undrained shear strength of the cohesive soil. The results of the tests on cohesive soil are summarized in the following table (note that the cohesive soil is generally dark, grey, stiff clay):

Depth (ft)	Unit Weight (lb/ft^3)	ϕ (deg.)	c_u (ksf)
0.5	126	0	3.0
	125	0	2.5
1.0	123	0	1.5
1.5	123	0	1.6
2.0	125	0	1.9
3.0	125	0	1.9

The cohesionless soil used was crushed limestone gravel. The soil properties at the site were determined by using a McGuin water pycnometer to obtain the in situ unit weight and by taking soil samples for laboratory testing.

Laboratory testing of the samples included sieve analysis and water content determinations. The gradation curve obtained from the sieve analysis is shown in Figure 3. The gravel was classified as a GW material by the Unified Soil Classification System. Because the maximum particle size of this material is too large to permit determination of the shear strength by using a standard triaxial compression test, the angle of shearing resistance was found from correlations with the gradation curve, maximum particle size, relative density, and the overburden pressure. These correlations were developed by Leps (3). From these correlations, a range of 48 to 52 degrees was chosen for the angle of internal friction. The properties of the cohesionless soil are summarized in the following table (note that the cohesionless soil is generally well-graded crushed limestone gravel):

Depth (ft)	Unit Weight (lb/ft^3)	ϕ (deg.)	c_u (ksf)
0.5	115	48-52	0
	115	48-52	0
1.0	120	48-52	0
1.5	120	48-52	0
2.0	125	48-52	0
3.0	125	48-52	0

Equipment and Instrumentation

In order to conduct these tests it was necessary to develop a loading system capable of (a) applying a horizontal force on the post at a uniform displacement rate, (b) measuring the load acting on the post at known displacements, and (c) measuring the displacement of the post at the ground surface. A hydraulic loading device was used to apply the lateral force to the posts. The loading system is illustrated in Figure 4. A hydraulic cylinder was attached to the concrete anchor and the post. The ram of the hydraulic cylinder was fully extended at the beginning of the test. A small hydraulic pump was used to retract the ram and to apply the load to the post.

The load applied to the post was measured by means of a force transducer attached between the post and the hydraulic cylinder, as shown in Figures 4 and 5. The transducer was calibrated up to a maximum load of 10,000 lb. The force transducer was constructed of a metal bar instrumented with a full bridge of strain gauges. The output from these strain gauges was measured with a digital microvoltmeter calibrated to read the load directly. For the static load tests, the post deflection at the ground surface was measured. Because the soil around the post deforms as the post is loaded, the post displacement must be measured from a fixed point some distance away from the post. A wooden stake was driven into the ground about 15 ft away from the

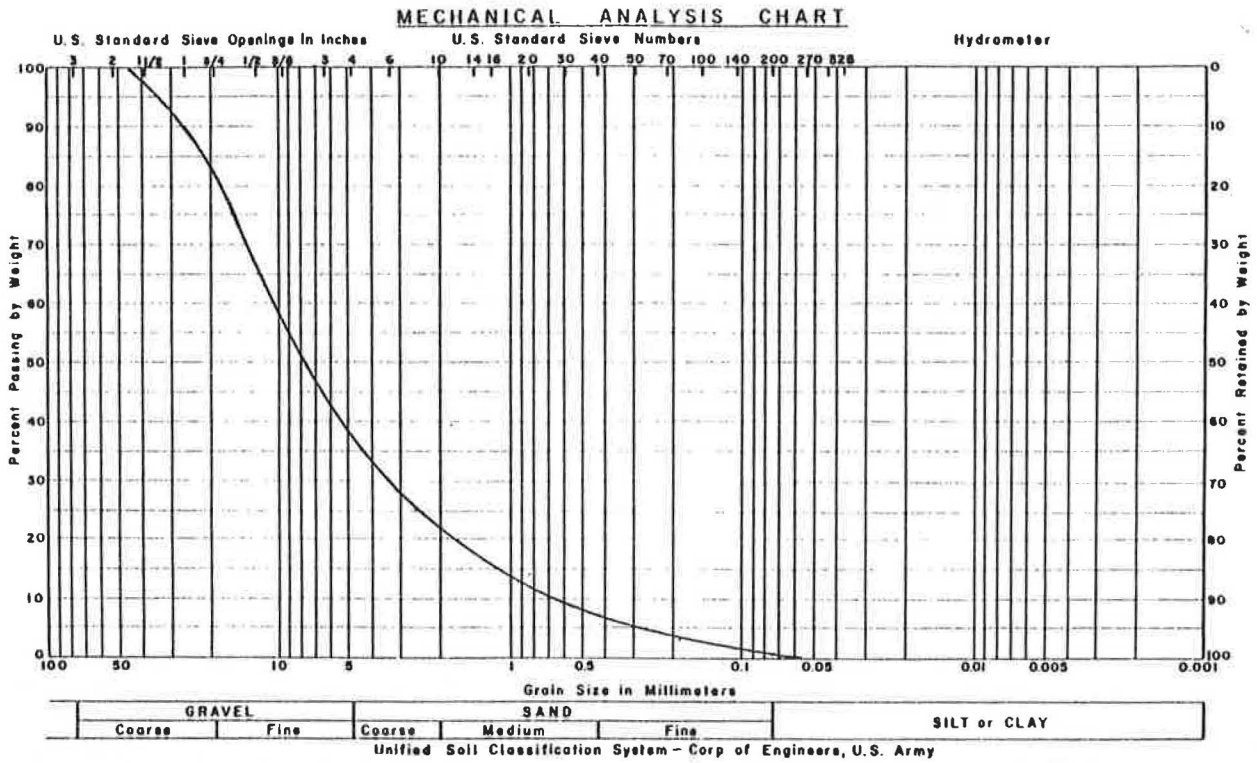

FIGURE 3 Gradation curve for the cohesionless soil.

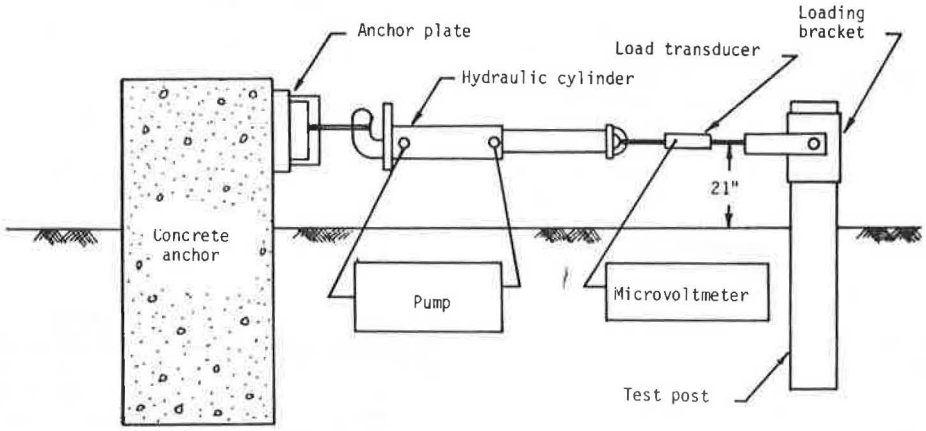

FIGURE 4 Lateral loading system.

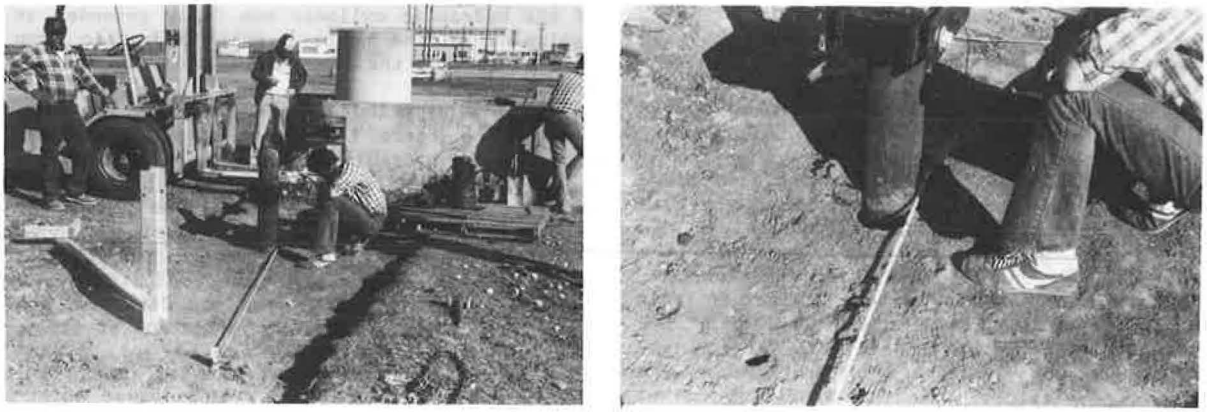

FIGURE 5 Measurement of post displacements.

post. A metal tape was attached to the stake and the post displacements were measured from this fixed point (see Figure 5).

Test Results

The results of the static guardrail post tests are shown in Figures 6-9 and are summarized in the following table (note that the entries under the Energy column give the energy dissipated after 18 in. of movement):

Test No.	Maximum Force (kips)	Force at 18-in. Movement (kips)	Energy (ft-kips)
1	3.7	3.7	4.2
2	3.3	3.3	3.8
3	3.8	3.8	4.3
4	3.2	2.9	4.4
5	3.3	3.2	4.2
6	3.9	3.9	5.2

The load-deflection curves for each test performed in the cohesive soil are given in Figures 6-8, and the load-deflection curves for the cohesionless soil are given in Figure 9. Maximum load values and dissipated energy values for all tests are given in the previous table. From the results of these static post tests, it is clear that the steel guardrail posts perform similar to the standard timber posts.

In the cohesive soil the steel post embedded 44 in. performed almost exactly as the timber post embedded the minimum 38 in. The steel post embedded 38 in. performed similarly to the wood post; however, there was a small decrease in both the maximum load and the energy dissipated. The decrease in the maximum lateral load was 11 percent, and the decrease in the energy dissipated was 10 percent.

In the cohesionless soil the lateral load capacity and the energy absorbed by the steel post embedded 44 in. were greater than those of the timber post. For the steel post embedded 38 in., the maximum load was 3 percent higher than the maximum load carried by the timber post; however, the energy absorbed by the steel post was 5 percent lower than the energy absorbed by the timber post.

Comparison of Test Results with Theoretical Predictions

The field load test results are shown in Figures 10 and 11, with the analytical results obtained by using the computer program LATPIL, which was developed during this study for two of the six tests.

The agreement between the analysis and the field load tests is satisfactory in all tests. In the cohesive soil the analytical results and the field test results match extremely well at ground-line displacements less than 4 in. A post displacement of 4 in. at the ground surface corresponds to a post rotation of about 10 degrees. For displacements in excess of 4 in., the post rotates a significant amount and the applied load tends to pull the post out of the ground. This axial pull on the post in-

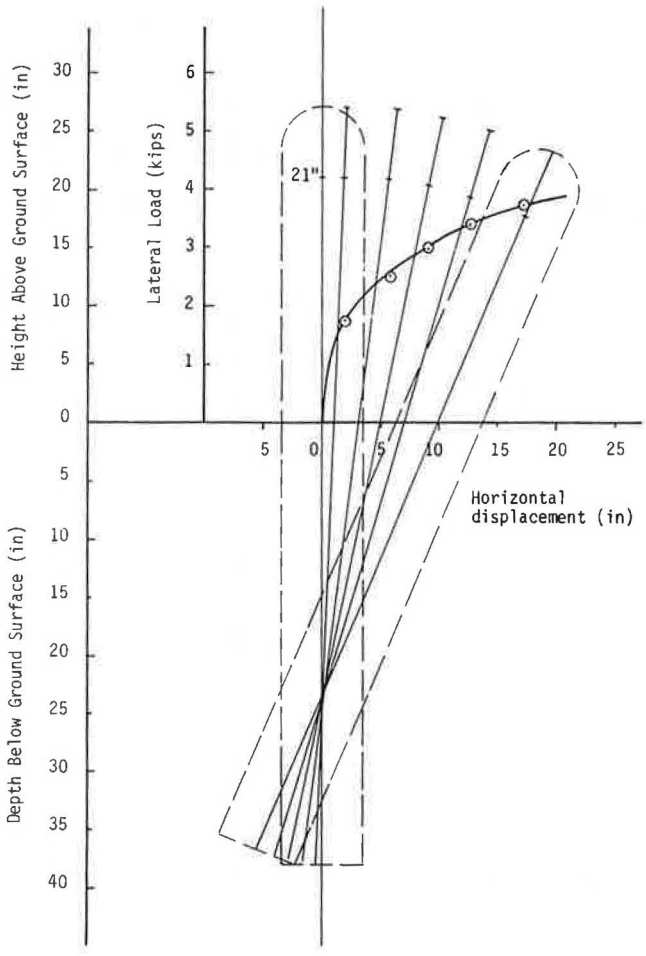

FIGURE 6 Lateral load versus deflection for post 1.

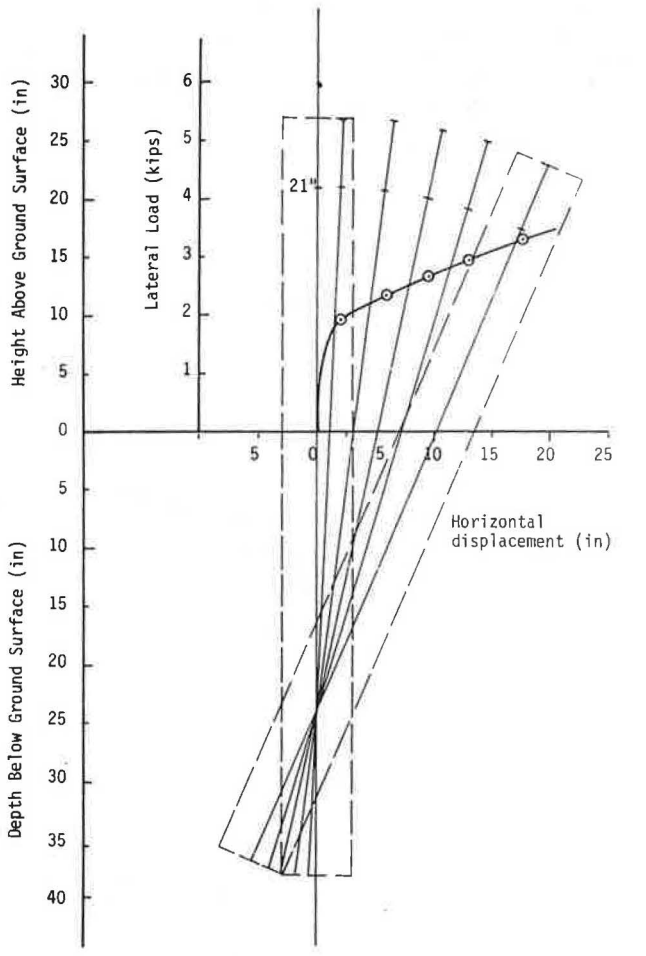

FIGURE 7 Lateral load versus deflection for post 2.

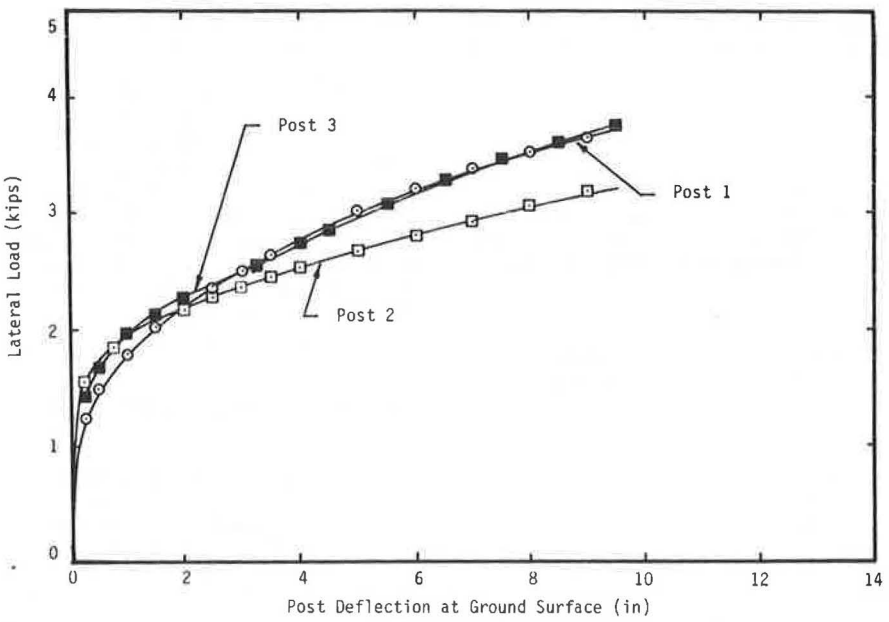

FIGURE 8 Static test results in the cohesive soil.

duces vertical shear stresses along the perimeter of the post, which tend to increase the lateral capacity of the post. For this reason the theoretical analysis underpredicts the lateral load for post displacements greater than 4 in.

In the cohesionless soil the theoretical predictions, given in Dewey et al. (2), agreed well with the field load tests. Both the shapes of the load-deflection curves and the maximum load values are predicted well by the model.

DYNAMIC LOAD TESTS

The dynamic load tests that were conducted are summarized in the following table:

Test No.	Post Type	Embedment Depth (in.)	Height of Rail (in.)	Soil Type
C1	Wood	38	21	Cohesionless
C2	Steel	38	21	Cohesionless
C3	Wood	38	21	Cohesive
C4	Steel	38	21	Cohesive

From the results of the static load tests, it was decided that dynamic load tests on the steel guardrail posts embedded 44 in. were not necessary. Both the static lateral load capacity and the energy dissipation capacity of the steel posts embedded 44 in. exceeded the capacities for the wood posts embedded 38 in. Although the dynamic behavior of the guard-

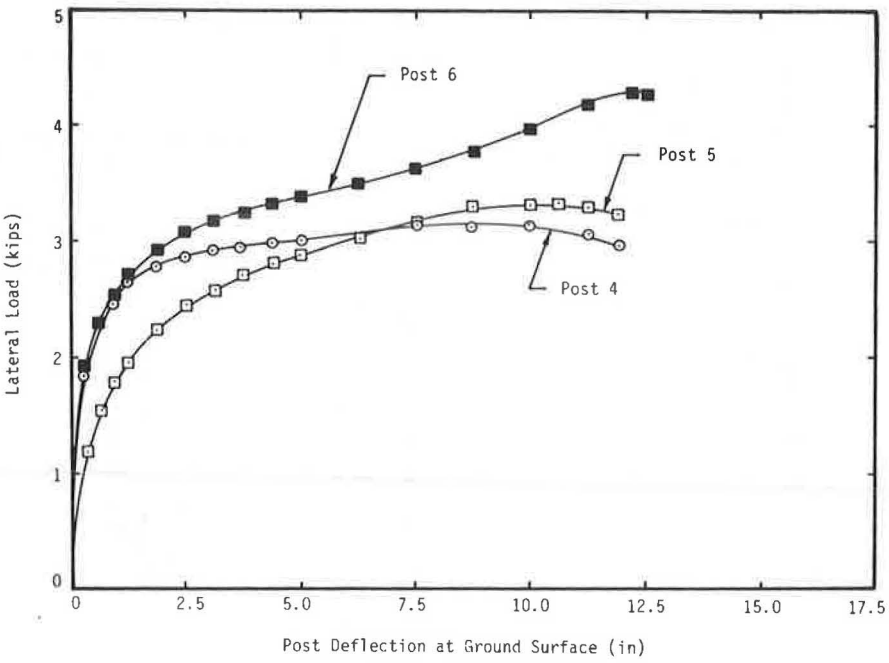

FIGURE 9 Static test results in the cohesionless soil.

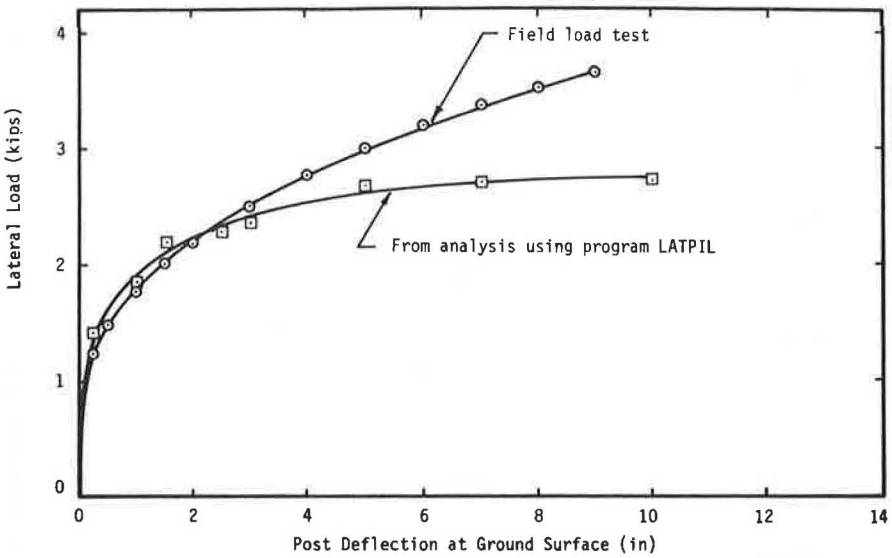

FIGURE 10 Comparison of analysis and field load test for post 1.

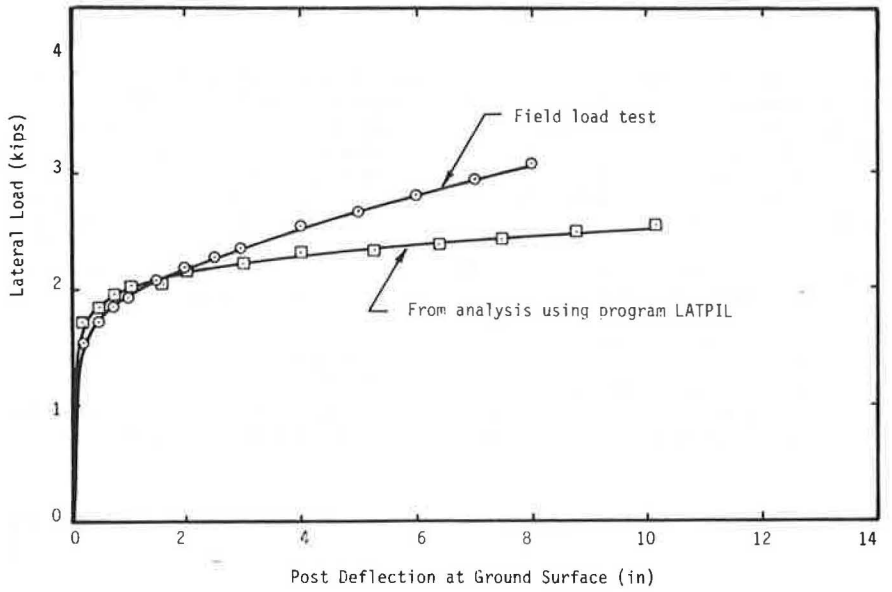

FIGURE 11 Comparison of analysis and field load test for post 2.

rail posts is quite different from the static behavior, the results of the static tests give a good indication of the relative performance of these posts.

Equipment and Instrumentation

Dynamic load testing of the guardrail posts requires systems capable of (a) dynamic load application, (b) dynamic load measurement, and (c) measurement of post deflection. The dynamic testing program was accomplished by using a cart of known mass to simulate an automobile. The cart shown in Figure 12 was used because of its extreme rigidity. Consequently, little energy is dissipated in deforming or crushing the cart itself.

The cart was positioned about 100 ft away from the posts. A cable was attached to the cart, placed around the pulley, and connected to a truck that pulled the cart into the post. A cable release mech-

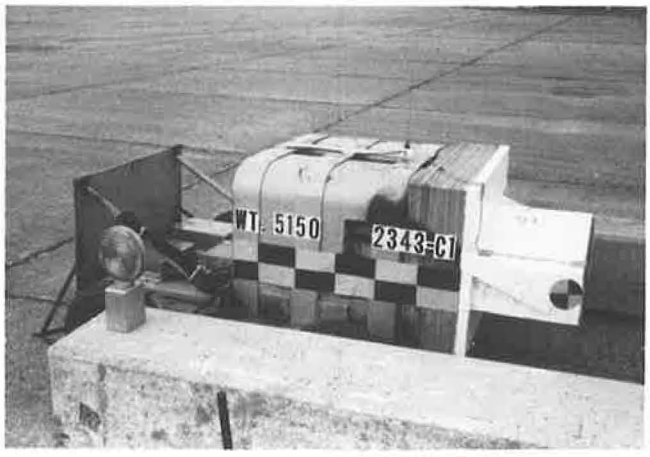

FIGURE 12 Automobile simulation cart.

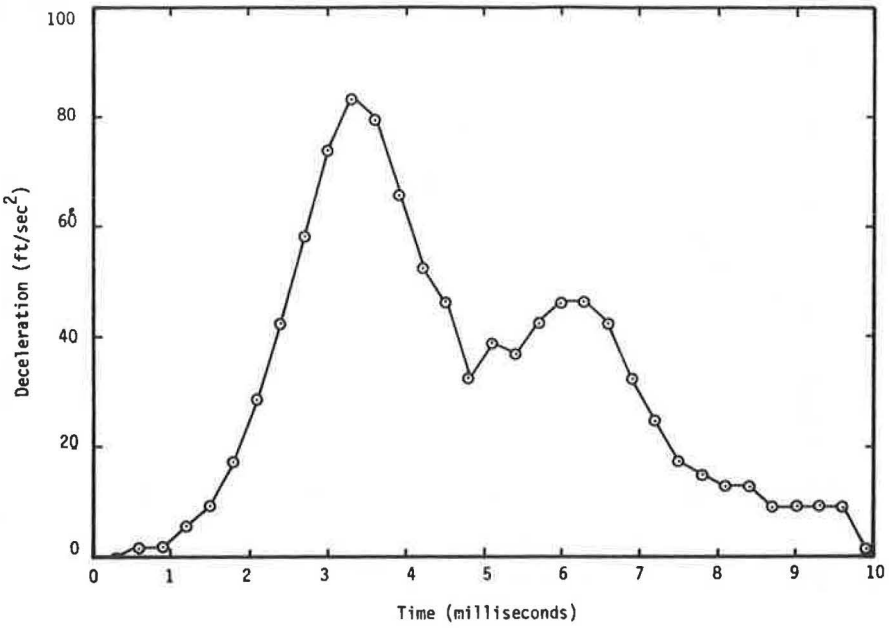

FIGURE 13 Cart deceleration versus time for test C1.

anism was placed directly ahead of the pulley to detach the cable from the cart. Because the cart has no means of steering, two concrete barriers were used to guide the cart toward the post.

The cart was instrumented with an accelerometer to measure the lateral deceleration during impact with the post. By knowing the mass of the cart, the lateral force applied to the guardrail post can be calculated by using the product of the cart mass and the cart deceleration. The accelerometer data were recorded by a computer every 0.0003 sec, and an output of force was obtained directly from this computer. Because the duration of the impact test is only a fraction of a second, direct measurement of the post displacement during the test is extremely difficult. However, the post displacement can be obtained indirectly by two methods. In the first method each test was photographed with a high-speed camera at a speed of 408 frames per second. The displacements of the post were scaled off the high-speed film. In the second method the post displacement can be calculated from the accelerometer data by integrating the deceleration-time curve twice. The cart velocity at the point of impact must be known for the second method; this was obtained from the high-speed film.

Test Results

The results from one of the four impact tests are shown in Figure 13. For each test, the results ob-

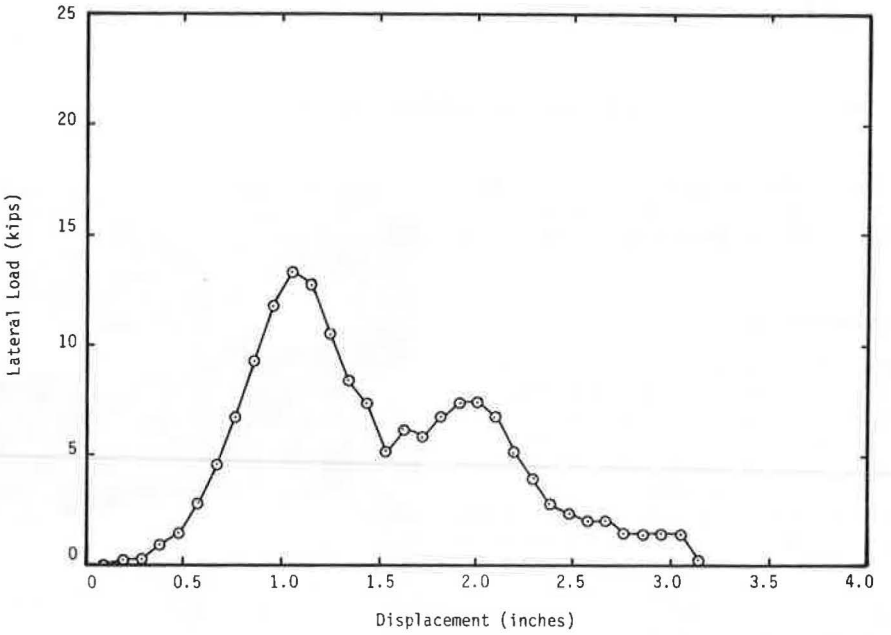

FIGURE 14 Lateral load versus post displacement for test C1.

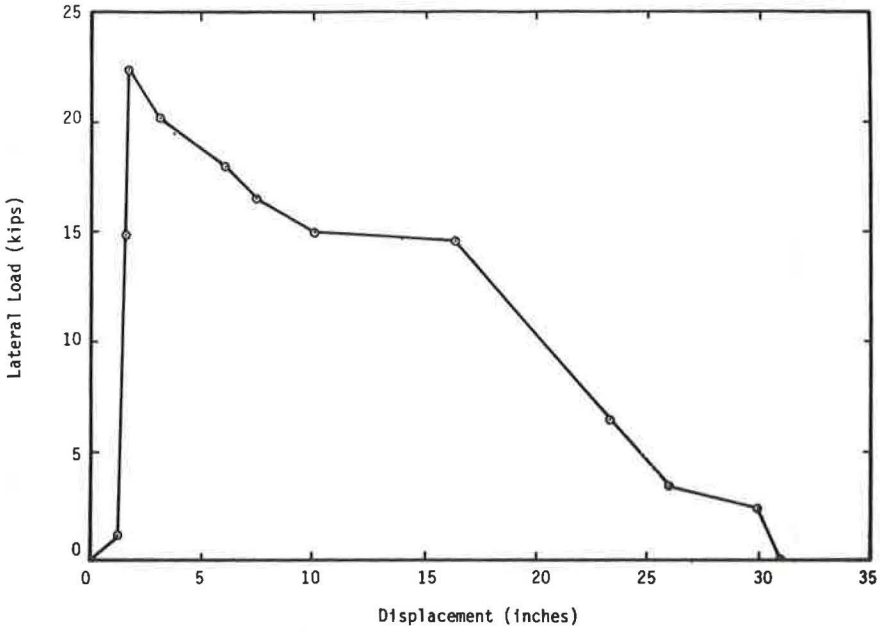

FIGURE 15 Lateral load versus post displacement for test C2.

tained include the deceleration-time curve, velocity-time curve, displacement-time curve, and load-deflection curve (see Figures 14-17). A comparison of the ultimate lateral load, dissipated energy, and the impact velocity for all four tests is given in the following table:

Test No.	Impact Velocity (ft/sec)	Maximum Force (kips)	Force at 18-in. Movement (kips)	Total Energy (ft-kips)
C1	26.6	13.3	-	1.3
C2	26.1	22.4	22.4	29.2
C3	22.7	16.3	19.2	27.2
C4	24.1	17.0	17.1	29.9

Note that the wood post in test C1 broke on impact with the cart. The post, however, had no visible signs of defects or cracks before the test. The maximum lateral load carried by the post was 13.3 kips. However, the wood post used in test C3 carried a lateral load of 16.3 kips without breaking. Thus, because of the nonhomogeneity of wood, the strength of the timber posts varies significantly. Because the post in test C1 broke during impact, a comparison of the steel and timber post in the cohesionless soil is not possible.

In the cohesive soil, the steel post (test C4) performed similarly to the timber post (test C3). The maximum lateral load carried by the steel post was 4 percent higher than the maximum lateral load carried by the timber post. The total energy dissipated by the steel post also exceeded the total

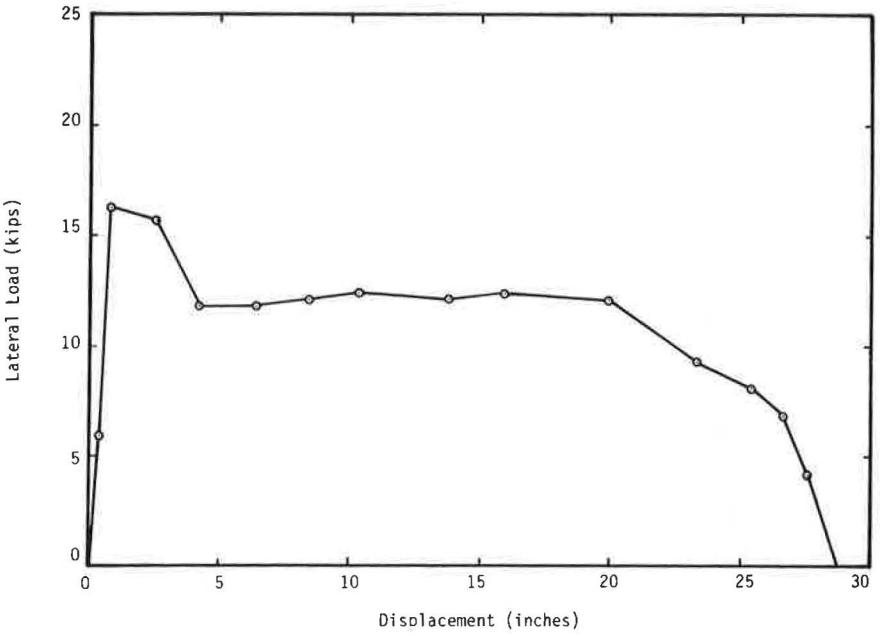

FIGURE 16 Lateral load versus post displacement for test C3.

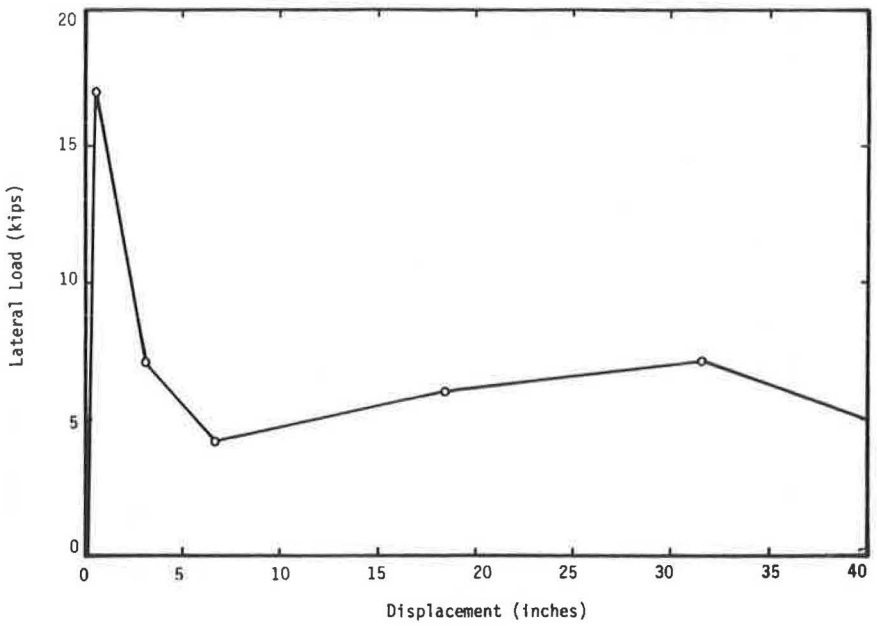

FIGURE 17 Lateral load versus post displacement for test C4.

energy dissipated by the wood post by 10 percent. Thus, based on the lateral load capacity and the total dissipated energy, the performance of the steel guardrail post actually exceeded the performance of the timber post.

Comparison of Test Results with Theoretical Predictions

Because the wood post broke during impact in test C1, a theoretical analysis was not performed. The analytical predictions obtained by using the computer program LATPIL are shown in Figure 18 with the field load test results for post C2. Because the viscosity of the soil cannot be determined easily, a range of values was used to obtain the analytical predictions. The range of viscosity values used for each of the tests was selected in order to bracket the field load test results. As shown in Figure 18, for test C2 the predicted load-deflection curves closely follow the field load test results.

CONCLUSIONS

The conclusions that can be drawn from this research study are as follows.

1. The analytical model developed during this research study can be used for the analysis of laterally loaded piles or drilled piers. The comparison of test results with the analytical predictions indicates that the analysis procedure developed is reliable for statically loaded drilled piers.
2. The static guardrail post tests conducted as part of this research study indicate that the steel guardrail posts embedded 38 in. without a concrete

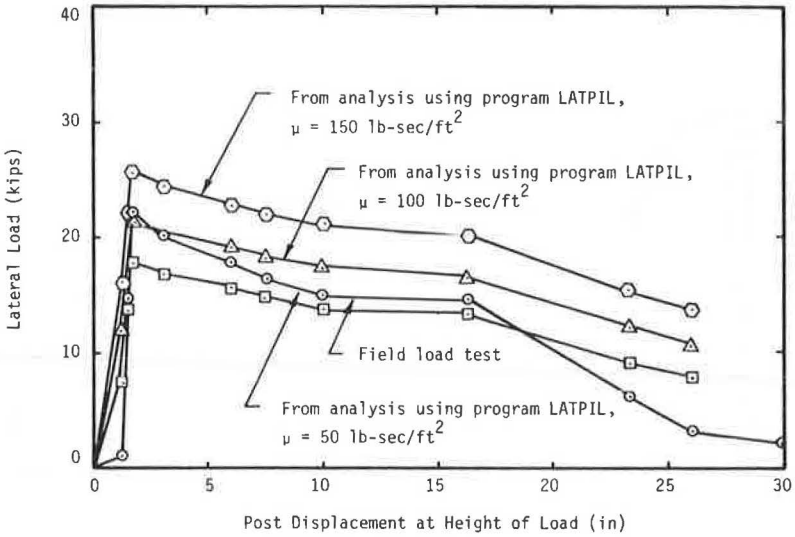

FIGURE 18 Comparison of analysis and field load test results for test C2.

footing performed similarly to the timber post embedded 38 in.

3. Comparisons of the static field test results with the analytical predictions indicate that the analytical model provides a useful means for predicting the response of guardrail posts to static loads.

4. The dynamic guardrail post tests conducted as part of this research study indicate that the steel guardrail post embedded 38 in. without a concrete footing performed similarly to the timber post embedded 38 in. Thus, based on the results of the limited field tests, the steel guardrail post embedded without a concrete footing performs satisfactorily as a traffic barrier system.

5. Comparisons of the dynamic field test results with the analytical model appear to provide a useful means for predicting the response of guardrail posts to dynamic loads. However, the analytical model is sensitive to the soil viscosity used in the dynamic model.

6. It should be emphasized, however, that these results and statements are based on a limited number of tests performed in the field on the steel and timber posts. Because of the limited time and resources available to the authors, repeatability of the test results was never verified. Therefore, it is recommended that another series of tests be performed in the future to check the repeatability of the results.

REFERENCES

1. Response of Guardrail Posts During Impact. Res. Report 03-9051. Southwest Research Institute, San Antonio, Tex., Oct. 1970.
2. J.F. Dewey, J.K. Jeyapalan, T.J. Hirsch, and H.E. Ross. A Study of the Soil-Structure Interaction Behavior of Highway Guardrail Posts. Res. Report 343-1. Texas Transportation Institute, Texas A&M University, College Station, July 1983.
3. T.M. Leps. Review of Shearing Strength of Rockfill. ASCE, Journal of the Soil Mechanics and Foundations Division, Vol. 96, No. SM4, July 1970.

Publication of this paper sponsored by Committee on Safety Appurtenances.

Encasement of Pipelines Through Highway Roadbeds: Synopsis of Final Report for NCHRP Project 20-7, Task 22

RAYMOND A. KOENIG, Jr.

ABSTRACT

Warrants for providing increased protection to pipelines crossing highways are discussed. The practice of using casing pipes to protect crossing pipelines is examined. Problems encountered with this practice, particularly related to interference with induced-current cathodic protection systems for pipelines, are presented. Two failures of pipelines, which the National Transportation Safety Board attributed to the use of casings, are documented. Results of a survey of state transportation departments, railroads, trade associations, utility companies, and pipeline operators are included.

In 1981 the Transportation Research Board, which administers the National Cooperative Highway Research Program (NCHRP), contracted Byrd, Tallamy, MacDonald and Lewis to conduct research addressing the need for encasing pipelines under highways. AASHTO sponsored the research in cooperation with the FHWA.

The objective of the research was to develop procedures for determining the need for pipeline encasement at highway crossings based on

1. A review of literature on underground pipeline design and performance,
2. Limited stress analyses of underground pipelines, and
3. An evaluation of field experience by highway, railroad, and utility agencies of encased and uncased pipelines.

The study was completed in late 1982, and the final report (1) has been accepted by NCHRP. Existing regulations concerning pipeline crossings are summarized, including those of the Office of Pipeline Safety, U.S. Department of Transportation. Forty-two publications relating to pipeline crossings are listed as references in the bibliography of the report. Results of a survey of state highway departments, utility companies, and pipeline operators regarding their encasement practices are presented. Problems encountered with the use of casings, particularly with regard to cathodic protection systems, are discussed. Warrants for providing